Tham Boi Chau
Akademia Morska w Gdyni

2-D VERSUS 3-D STRESS ANALYSIS OF A MARINE PROPELLER BLADE

The shapes of propeller blades are built from two-dimensional data of blade cross sections. The stress field of propeller blades are analyzed basing on the results of three-dimensional models and, previously, on beam models. In this paper the possibility of applying the theory of thin shells for this purpose is discussed.

INTRODUCTION

Stress analysis of marine propellers presents unique difficulties due to complicated, doubly curved, shape of the blades that have to be accounted for with considerable accuracy. Even with the stage of geometric modelling completed, there is still the question which of the mechanical models to choose for subsequent stress analysis. Prior to the ascent of numerical techniques based on automated computing, the beam theory was generally used for this purpose (see [2, 4, 6]). This approach seems unjustifiably crude nowadays though. Undoubtedly, the most reliable results can be obtained from 3-D analysis [4]. Yet for reasons to be explained elsewhere, application of a 2-D shell model is worth considering.

This work will focus merely on the process of creating 3-D model of propeller blades for purposes of structural analysis. It seems it is best to follow here the traditional method of designing marine propellers, wherein one obtains design data in the form two-dimensional data tables of blade cross sections. But with such data it is still difficult to picture the real shape of propeller blades.

An equivalent 2-D model is also created from those data. Both models are then solved numerically by the Finite Element Method [16] with the help of MD Nastran®. 3-D model is analyzed basing on the classical theory of deformable solids, whereas for the 2-D model the classical theory of thin shells is used. Finally, the comparison of results obtained from solving 3-D and 2-D models is carried out.

1. 3-D MODEL OF A PROPELLER BLADE

1.1. Blade description

The description of the geometry of marine propeller blades can be found in many references (see e.g. [2, 4, 6, 15, 17, 18]). Here we only recall some conventions to which we will consistently stick throughout this work. Henceforth, we will refer to the right handed propellers only. Therefore, the figures presenting blades or propellers show the leading edge to the right. However, where only radial cross-sections are presented, they are shown with the leading edge to the left in accordance with the general convention adopted for drawing airfoils [1].

The orientation of the global right handed XYZ Cartesian system follows these rules (see fig. 1). The *Z* axis is aligned with the symmetry axis of the propeller and is directed aft. The *Y* axis is perpendicular to *Z* and aligned with the axis about which a controllable pitch blade would be rotated to change pitch (although no assumption is made that the propeller is actually a controllable one). Additionally we assume the *Y* axis aims up and, thus, the *X* axis aims starboard.

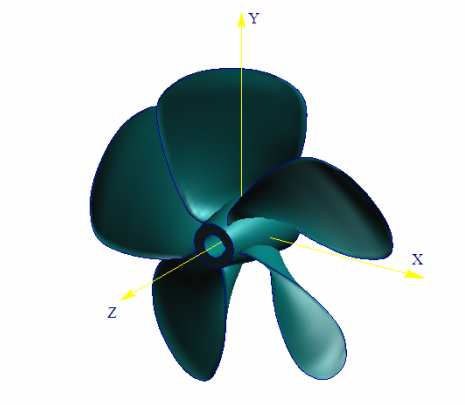

Fig. 1. Right handed propeller and convention coordinate system

1.2. Generation of Spatial Coordinates

Specific data of the blade analyzed in this work are contained in table 1. There *XC* denotes the ratios between abscises and chord, *XL* denotes the distance from leading edge, *YG* denotes the suction side ordinate, *YD* denotes the pressure side ordinate, RR denotes the ratio of radii, *RLE* denotes the leading edge radius and *RTE* denotes the trailing edge radius of the blade cross section.

Table 1

Blade section coordinates

XC	0.0	0.0125	0.025	0.05	0.10	0.20	0.30	0.40	0.50	0.60	0.70	0.80	0.90	0.95	1.00
RR = 0.2500 *RLE* = 0.0061 *RTE* = 0.0037															
XL	0.0	0.0281	0.0563	0.1125	0.2251	0.4502	0.6752	0.9003	1.1254	1.3505	1.5755	1.8006	2.0257	2.1382	2.2508
YG	0.0	0.0364	0.0610	0.0958	0.1507	0.2323	0.2864	0.3183	0.3285	0.3179	0.2831	0.2214	0.1294	0.0710	0.0187
YD	0.0	0.0225	0.0334	0.0420	0.0487	0.0511	0.0485	0.0465	0.0454	0.0461	0.0453	0.0402	0.0274	0.0172	0.0187
. . . . .															
RR = 0.9750 *RLE* = 0.0055 *RTE* = 0.0003															
XL	0.0	0.0252	0/0504	0.1008	0.2016	0.4031	0.6047	0.8063	1.0079	1.2094	1.4110	1.6126	1.8142	1.9149	2.0157
YG	0.0	0.0051	0.0092	0.0158	0.0270	0.0448	0.0571	0.0644	0.0668	0.0644	0.0568	0.0438	0.0251	0.0135	0.0017
YD	0.0	0.0003	-0.0005	-0.0031	-0.0087	-0.0188	-0.0264	-0.0310	-0.0325	-0.0310	-0.0267	-0.0198	-0.0107	-0.0054	0.0017

Basing on these data we can draw the blade section in a coordinate system in accordance with airfoil conventions. For example, the following figure 2 presents the full developed section of the blade at the radius ratio of 0.25

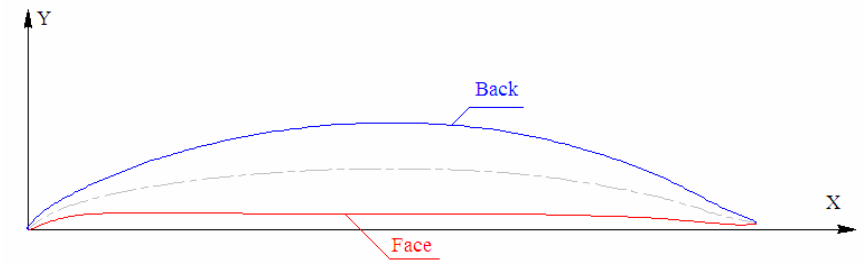

Fig. 2. A Blade Section in the Airfoil coordinate system

The spatial coordinates for propeller blade are generated by transforming the 2-D coordinates of the expanded view and the blade sections into three-dimensional coordinates of the blade in its final forms (fig. 3). The fully developed sections in the expanded view show skew as an offset *SK* of the mid chord from the *Y* axis. In some cases, the point of maximal thickness is used rather than the mid chord point. If the blade has rake, the unwrapped sections on the *XY* plane are offset a distance along the *Z* axis, an amount equal to the rake *RK*. Each section is

rotated about the point of intersection of the mid chord line with the *YZ* plane to its specified pitch angle ϕ, measured between the pitch chord line and the *XY* plane. Angles measured counter-clockwise from the *XY* plane are positive. If there is no rake, the projection of the line on the *XZ* plane runs through the origin of the *XZ* system, which becomes the centre of the pitch rotation. The coordinates of the face and back can be transformed to the global *XYZ* system using the following equations and keeping in mind that *TB* and *TF* are negative above the chord line and positive below.

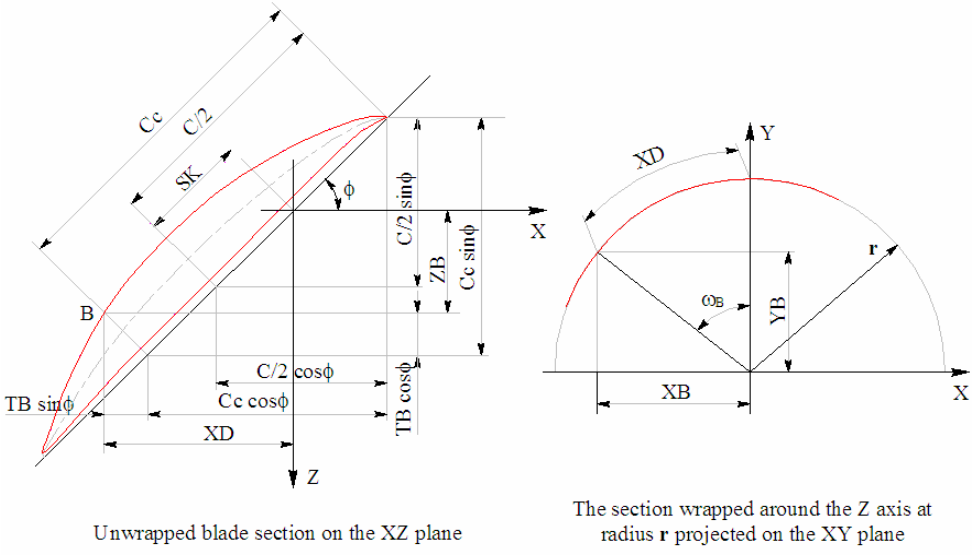

Fig. 3. Generation of spatial *XYZ* coordinates

For points lying on the face and back of the blade section which have coordinates $X < 0$ (points are in the left of the *Z* axis on the *XZ* plane in figure 3), the spatial coordinates of these points are computed as follows

$$ZB = SK\,\sin\phi + C\left(c - \frac{1}{2}\right)\sin\phi - TB\,\cos\phi\,, \tag{1}$$

$$\omega_B = \frac{1}{r}\left[SK\,\cos\phi + C\left(c - \frac{1}{2}\right)\cos\phi + TB\,\sin\phi\right], \tag{2}$$

$$XB = -r\,\sin\omega_B \tag{3}$$

$$YB = r\,\cos\omega_B \tag{4}$$

On the other hand, for the points lying on the face and back of the blade section which have coordinates $X > 0$ (points are in the right of the *Z* axis on the *XZ* plane in figure 3), the spatial coordinates are computed as follows

$$ZB = SK\,\sin\phi + C\left(c - \frac{1}{2}\right)\sin\phi - TB\,\cos\phi \tag{5}$$

$$\omega_B = \frac{1}{r}\left[SK\,\cos\phi + C\left(c - \frac{1}{2}\right)\cos\phi + TB\,\sin\phi\right] \tag{6}$$

$$XB = r\,\sin\omega_B \tag{7}$$

$$YB = r\,\cos\omega_B \tag{8}$$

Using the formulas from (1) to (8) we can compute spatial coordinates of points on the face and back of each blade cross section automatically from design data using a MATLAB® routine.

1.3. The analysis models of the blade

Having generated spatial coordinates of cross sections, we can create the models for analyzing the structure and then use PATRAN® pre/postprocessor to visualize the models and the results. For example, table 2 shows the design data of a marine propeller obtained from a team in IFFM of the PAScie in Gdańsk.

Table 2

Principal characteristics for fixed propeller thrust blade section profile NACA65

Number of blades	5	Wake fraction	0.3160
Diameter (M)	7.0000	Rake (DEG)	0.0000
Hub Diameter (M)	1.4000	Skewback (DEG)	4.8991
Design Speed (W)	22.0000	Blade Area Ratio	0.9750
Revs. Per minute	91.0000	Thrust (N)	2748202.0000
Shaft Immersion (M)	4.5000	Power (KW)	38741.8945
Wat. Densc (KGM^{-3})	1025.0000	Advance Coef.	0.7285
Cavit. Number	2.4936	Thrust Coef.	0.4855
Tip Vortex Kernel (MM)	138.2382	Torque Coef.	0.1027
Coef. Of Distr. Circu	0.5409	Efficiency	0.5484

After generating spatial coordinates from two-dimensional data tables of blade cross sections we build 3-D geometric model of the propeller blade which is created from solid elements (HEXA, PENTA and TETRA elements). Figure 4a shows PATRAN visualization of the model. A 2-D model of the same propeller blade is also created from 2-D QUARD4 and TRIA3 elements (see fig. 4b).

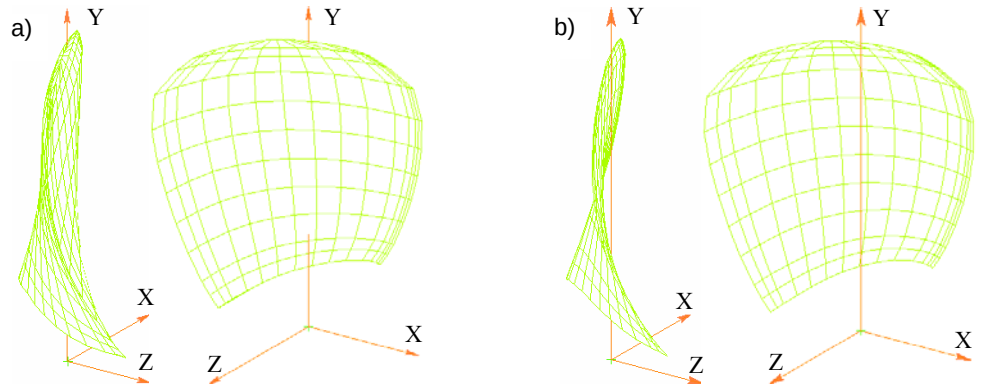

Fig. 4. Geometrical models of the propeller blade

To solve these models with MD Nastran®, we need to prescribe the material properties, boundary conditions and loads acting on the blade. It is assumed the blade is clamped at the root section (where the blade intersects with the propeller hub), and is subject to the action of pressure loads arising from water flow on both sides of the blade, and also to centrifugal forces due to rotational velocity of the propeller (see e.g. [2, 6, 8, 15, 17]). As to the material properties, it is assumed the blade is made up of high tensile brass with Young modulus $E = 7 \cdot 10^{10}$ (Pa), Poisson ration = 0.33 and density $\rho = 8 \cdot 10^{3}$ (KGm^{-3}).

Figure 5 presents the distribution of the pressure acting on the face of the blade. These values are obtained from design data of the marine propeller.

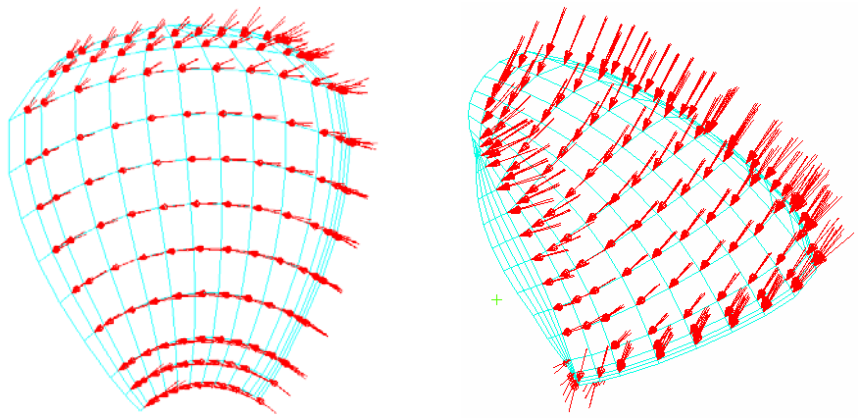

Fig. 5. Distribution of pressures on the face of the 3-D model

The figures 6 and 7 show graphically the results of several runs of MD Nastran® on both models of the blade.

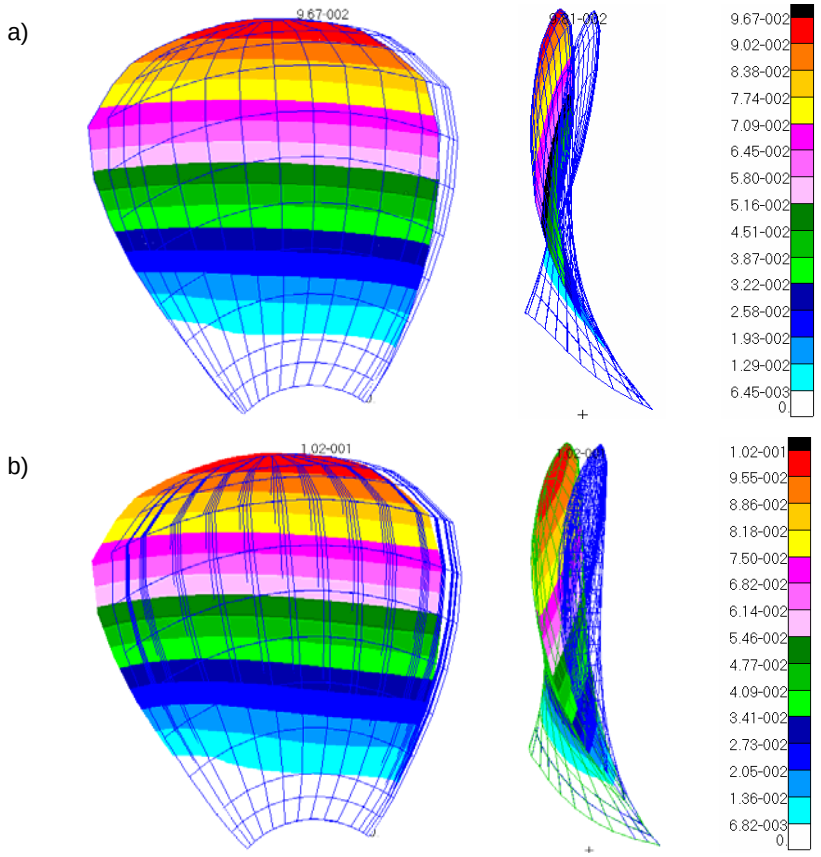

Fig. 6. Displacement field of 2-D model (a) versus 3-D model (b)

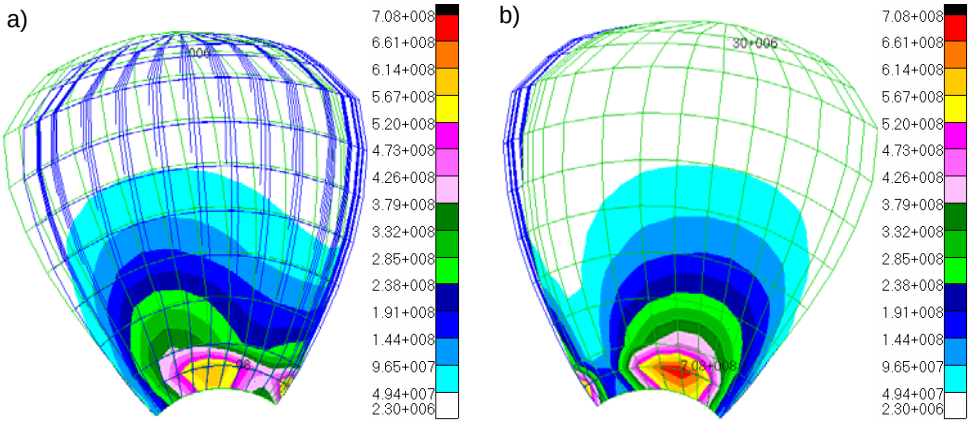

Fig. 7. Distribution of stress on the Face (a) and Back (b) of the 3-D model

2. ANALYSIS OF THE RESULTS

The figures 6a and 6b present the displacement fields of the 2-D model, and 3-D model, respectively. We can recognize the similarity in the distribution of displacement field in both models. The maximum value of the displacement of the 2-D model is about 5.19% smaller than its counterpart of the 3-D model. The displacements in the region close to the root section of the blade are very small. The displacement field increases along the propeller radius assuming the largest values near the tip. Within a fixed blade cross section the displacement field decreases from the leading edge to the trailing edge.

The distribution of the stress on the face and back of 3-D model is presented in the figure 7. As one might expect, the results show that the stresses reach values in the region near the root section around the leading edge. The stress field decreases with the growing values of the radius and drop to small values in the region near the tip of the blade. Such distributions of the displacements and the stresses seem realistic in comparison to what is observed in practice, because the blades are fixed in the propeller hub at their root sections and bent by the difference of pressures between their face and back sides.

The classical method of calculating the strength of propeller blades based on the beam theory (Taylor's Method) also shows that the maximum stresses in the propeller blade occur in the region around the root section of the blade [2, 4, 6]. The newer method using theory of shells of moderate thickness for solving thick finite element model (see [6, 8]) also results in the distribution of the stress field similar to the results obtained from our computations.

CONCLUSION

Solving the 3D model of propeller blade basing on the classical theory of deformable solids shows us the values of the stress and displacement fields in the blade. From that we can know the maximum displacement and stress and we can estimate the strength reliability of the propeller. When the blades are deformed, (that is, their geometry is changed) the hydrodynamic properties (as angles of attack, distribution of pressures on back and face surface etc.) of cross sections also change. Changing hydrodynamic properties of blades alters the efficiency of the propeller during the operation. If we know about these changes we can limit or eliminate the unfavorable changes by correcting or improving the geometry of the blade already at the design stage. Since the alteration of the geometry results principally from bending of the blade (stretching due to centrifugal forces contributes only a secondary effect), and 3-D approach does not account directly for bending as an independent deformation component, it seems reasonable to base the analysis on a theory of shells rather than the theory of 3-D deformable body. In practical

terms a propeller blade is a curved shell of variable thickness. Unfortunately, the theory of shells of variable thickness has not been completed yet, nowadays [3, 19]. For now a 2-D model based on the classical theory of thin shells [4, 5, 6, 7, 8] for propeller blades must satisfy our requirements. The results of the case study discussed in this work seem to substantiate the anticipation that a 2-D approach can yield reliable basis for analysis of this kind.

REFERENCES

1. Abbott I. H., von Doenhoff A. E., *Theory of Wing Section*, Dover, New York 1959.
2. Bauer G., *Marine Engines and Boilers*, Crosby Lockwood and Son 1905.
3. Berger N., *Estimates for Stress Derivatives and Error in Interior Equations for Shells of Variable Thickness with Applied Forces*. SIAM Journal on Applied Mathematics, SIAM, 1973, vol. 24, pp. 97–120.
4. Carlton J., *Marine Propellers and Propulsion*, Butterworth-Heinemann 2007.
5. Flügge W., *Tensor analysis and continuum mechanics*, Springer-Verlag, Berlin-Heidelberg-New York 1972.
6. Jarzyna H., Koronowicz T., Szantyr J., *Design of Marine Propellers*, „Maszyny Przepływowe", t. 20, 1996.
7. Koiter W.T., *A consistent first approximation in the general theory of shells*, In The Theory of Thin Elastic Shells. Proceedings of the IUTAM Symposium, Delft, 1959, Amsterdam, North Holland, 1960, pp. 12–33.
8. Koronowicz T., Krzemianowski Z., Tuszkowska T., Szantyr J.A., *A complete design of ship propellers using the new computer system*, Polish Maritime Research, 2009, 1(59), vol. 16, pp. 29–34.
9. MSC. Nastran 2003 Linear Static Analysis User's Guide.
10. MSC. Nastran 2004 Reference Manual.
11. MSC. Nastran 2008 Quick Reference Guide.
12. MSC. Patran MSC. Nastran Reference Guide, vol. 1, Structural Analysis.
13. MSC. Patran User's Guide.
14. MSC. Patran Reference Manual.
15. Muckle W., *Naval Architecture for Marine Engineers*, Newnes-Butterworths, London 1975.
16. Oden J.T., *Finite Elements of Nonlinear Continua*, McGraw-Hill 1972.
17. Rawson K.J., Tupper E.C., *Basic Ship Theory*, vol. 2, Butterworth-Heinemann 2001.
18. Smith D. R., Slater J. E., *The Geometry of Marine Propellers*, Report of Defence Research Establishment Atlantic, 1988.
19. Szwabowicz M.L., *Towards the theory of shells of variable thickness*, [in:] *Shell Structures: Theory and Applications*, vol. 2, eds: W. Pietraszkiewicz, I. Kreja, CRC Press 2009, pp. 99–102.

DWU- I TRÓJWYMIAROWA ANALIZA WYTRZYMAŁOŚCIOWA SKRZYDŁA OKRĘTOWEJ ŚRUBY NAPĘDOWEJ

Streszczenie

W pracy omówiono rezultaty analizy wytrzymałościowej skrzydła okrętowej śruby napędowej. Analizę przeprowadzono za pomocą metody elementów skończonych. Zastosowano model trójwymiarowy oraz dwuwymiarowy (powłokowy) i porównano wyniki otrzymane dla obu podejść do tego problemu.